

Soft Condensed Matter Perspective on Moisture Transport in Cooking Meat

R. G. M. van der Sman

Agrotechnology and Food Sciences, Wageningen University, 6700 AA Wageningen, The Netherlands

DOI 10.1002/aic.11323

Published online September 27, 2007 in Wiley InterScience (www.interscience.wiley.com).

We have viewed cooking meat from the perspective of soft condensed physics and posed that the moisture transport during cooking can be described by Flory-Rehner theory of swelling/shrinking polymer gels. This theory contains the essential physics to describe the transport of liquid moisture due to the denaturation and shrinkage of the heated protein matrix. The validity of our hypothesis is shown by a numerical model, which comprises a linearization of the Flory-Rehner theory augmented with Darcy's law for porous media flow, applied to the simulation of cooking experiments performed on a rectangular piece of beef. Reasonably, comparable results are obtained from simulations and experiments. Further analysis of simulations resolves yet another unexplained phenomena observed during heating of meat. Literature review suggests that Flory-Rehner is applicable to cooking of other gel-like foods. © 2007 American Institute of Chemical Engineers AIChE J, 53: 2986–2995, 2007

Keywords: food, porous media, mass transfer, thermodynamics/classical

Introduction

The physics behind the moisture transport during cooking of meat are yet poorly understood. In literature, there exist several models approaching this problem,^{1–7} which are based on Fickian diffusion of moisture. This type of model is very common place in the field of food engineering, despite the fact that it cannot be justified from physical considerations.^{8,9} Especially, it fails to capture the pressure-driven flows that definitely occur during the cooking of meat.^{10–12}

In this study, we have viewed the cooking of muscle meat from the perspective of the physics of soft condensed matter,^{13,14} and we pose that the pressure-driven moisture transport can well be explained from the Flory-Rehner theory of swelling or shrinking polymer gels. We have formulated our hypothesis as a numerical model. It has the complexity of models more commonly used in chemical engineering, which is rarely found in the field of food science—with notable exception of models by Datta and coworkers.^{8,15,16} Therefore, we view it important to communicate our model to the field of chemical

engineering. Furthermore, we like to make researchers in this field aware of the fascinating physics of food matter.

Because meat is probably an unusual matter for the readers, we first review some earlier descriptive works from the field of food science on moisture transport in cooking meat. Subsequently, we look at the moisture transport during cooking from the viewpoint of soft condensed matter and the Flory-Rehner theory in particular.

To further illustrate the physics during cooking, a numerical model is build, thereby using a linearization of Flory-Rehner theory. The model is used to predict the moisture transport during cooking of a rectangular piece of beef, for which the valuable data are available in literature.

After having validated that Flory-Rehner model applies, we have investigated moisture transport in more detail and resolved yet another unexplained phenomena reported in literature of meat cooking.

Theory

Moisture transport in cooking meat

An early qualitative model for liquid moisture transport in cooking meat, with a surprisingly good description of under-

Correspondence concerning this article should be addressed to R. G. M. van der Sman at ruud.vandersman@wur.nl.

lying physics, has been formulated by Godsalve et al.¹¹ Their model says that during cooking, the muscle proteins denature, leading to a decrease in their water holding capacity (WHC) and shrinkage of the protein network. This shrinking network exerts a mechanical force on the excess water. If pressure gradients are present, the excess water is expelled to the surface of the meat. The expelled water is commonly known as cooking losses. Today, the hypothesis of Godsalve et al. is still accepted as a valid (qualitative) description of moisture transport during the cooking of meat.^{12,17}

Until now, a physical sound, quantitative model has been lacking. As mentioned earlier, all earlier numerical models on moisture transport have been formulated using the moisture diffusion model, which lumps all different moisture transport phenomena such as capillary transport and gas pressure-driven flow, into moisture diffusion.⁸ The moisture diffusion model forbids transport against moisture content gradients, but this has been observed during meat cooking via NIR measurements of local moisture content in the center of the meat during heating.^{10,18} Recently, it has been recognized that this moisture rise in the center of meat is a real physical effect and is due to pressure-driven flows.¹² It is ruled out that the moisture transport in cooking meat is a Fickian diffusion process.^{10,12} A more complex, Luikov type of model¹⁹ takes into account the coupling between temperature and moisture transport via quasi-Soret/Dufour effects. Despite that it can be shown that the Luikov model is mathematically equivalent with our model presented below, the model is phenomenological in nature and does not provide any physical insight.⁸

Hence, for finding a physically based quantitative model for the moisture transport, we need to search outside the field of meat science. We have conjectured that the processes described by Godsalve et al.¹¹ are quite reminiscent to processes occurring during syneresis of cheese curd^{20–22} and polymer gels.^{23–25}

Early models of curd syneresis^{20,21} follow the Biot's model of fluid transport in poroelastic materials. A recent model²² follows more developed poroelastic models. In this type of model, pressure-driven flow is described by Darcy's law, commonly used in regular porous media research. In poroelastic media, the pressure on the fluid is partly due to the deformation of the elastic solid matrix. In cheese ripening, the solid matrix contracts due to the action of pH and enzymes. Since the poroelastic theory does not provide a constitutive equation for the pressure, a phenomenological equation is formulated for cheese.²²

Polymer gel syneresis and moreover the reverse process, swelling, have been widely investigated.^{23–26} Modeling approaches of swelling have been reviewed recently.²³ In these models, the swelling equilibrium is described via the thermodynamic theory of Flory-Rehner. The Flory-Rehner theory is expressed in terms of the Gibbs free energy. Formulation of thermodynamics of soft matter, which includes polymers, in terms of free energy has become a powerful instrument in soft matter physics, and we view it likewise for foods, being a quite complex soft matter.^{13,14} We have successfully applied free energy approaches to the surfactant-stabilized emulsions.^{27,28}

Flory-Rehner theory extends the Flory-Huggins free energy functional for polymer-solvent mixtures with an elastic term,

which account for the crosslinks existing between the polymers in the gel. From the free energy, a (swelling) pressure can be derived, which can be inserted in the momentum transport equation, e.g., Darcy's law.²³

Reinvestigation of quite early polymer and biophysics literature has shown that Flory-Rehner or related theories have been proposed for (muscle) proteins gels^{29,30} and even for muscle.^{31–33} These findings have us made the hypothesis that Flory-Rehner theory also holds for cooking meat. Details of the Flory-Rehner theory and how it applies to cooking meat are discussed in the next section.

Flory-Rehner theory

The Flory-Rehner theory is a statistical thermodynamic model, describing the free energy of elastic polymer gels, and has been extended to polyelectrolyte gels.²³ It has been considered to hold for muscle fibers,^{31,32} which can be viewed as a regular network of polyelectrolytes in an ionic solution.³³ For polyelectrolyte gels, the free energy has three contributions:

$$F = F_{\text{mix}} + F_{\text{el}} + F_{\text{es}} \quad (1)$$

where F_{mix} the free energy of mixing the polymer with solvent (i.e., water), F_{el} the free energy of elastic deformation of the gel, and F_{es} is the electrostatic contribution.

From the free energy functional Eq. 1, thermodynamic potentials can be derived like pressure, electrostatic, and chemical potential. If gradients in these potentials exist, there will be transport of ions, solvent, or polymer (in which case one speaks of deformation), until the equilibrium is restored.

The pressure derived from the Flory-Rehner free energy functional is the driving force for moisture transport in muscle meat. As is customary in polymer physics, we name this pressure the swelling pressure π_{sw} . The swelling pressure has three contributions:

$$\pi_{\text{sw}} = \pi_{\text{mix}} - \pi_{\text{el}} + \pi_{\text{es}} \quad (2)$$

With the mixing or osmotic pressure π_{mix} derived from F_{mix} , the elastic or network pressure π_{el} derived from F_{el} , and π_{es} the electrostatic contribution. In equilibrium, the swelling pressure is zero $\pi_{\text{sw}} = 0$.

In the original Flory-Rehner theory, the contributions to the swelling pressure read²³:

$$\pi_{\text{mix}} = + \frac{\partial F_{\text{mix}}}{\partial \phi} = \frac{RT}{V_w} [\ln(1 - \phi) + \phi + \chi \phi^2] \quad (3)$$

and

$$\pi_{\text{el}} = - \frac{\partial F_{\text{el}}}{\partial \phi} = RT \frac{\rho_p}{\bar{M}_c} \left[\frac{1}{2} \phi - \phi^{1/3} \phi_0^{2/3} \right] \quad (4)$$

where ϕ is the volume fraction of the polymer, T is the absolute temperature, R the gas constant, χ is the Flory-Huggins interaction parameter, V_w is the molar volume of the solvent, ρ_p the density of the polymer, \bar{M}_c the average molar weight of polymer segments in between crosslinks, and ϕ_0 the polymer fraction at crosslinking.

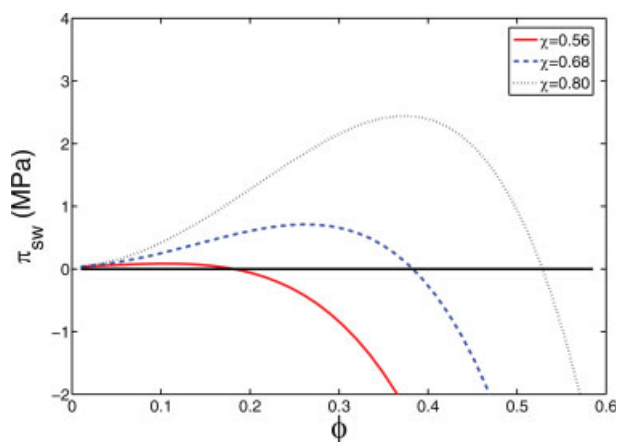


Figure 1. Sample plots of swelling pressure π_{sw} versus protein volume fraction ϕ for (a) $\chi = 0.56$, 0.68, and 0.80 (left to right).

[Color figure can be viewed in the online issue, which is available at www.interscience.wiley.com.]

The electrostatic contribution in the swelling pressure π_{es} also scales with ϕ^2 , and in case of uniform charge distribution its action can be absorbed in the interaction term of the osmotic pressure that is linear in χ .³² This approach can also be used for cooking meat.

Some values of parameters in the free energy functional can be found in literature. For skinned muscle fibers³² $\chi \approx 0.5$ and for elastin³¹ (a muscle-borne protein) $M_c = 6$ kg/mol. The density for proteins is about $\rho_p = 1300$ kg/m³. We have taken the volume fraction of proteins in raw meat $\phi_0 \approx 0.17$. The value of the Flory-Huggins interaction parameter χ is quite similar to other proteins³¹ and polysaccharides like starch.³⁴

Upon heating above 40°C meat proteins denature and uncoil, exposing more hydrophobic parts to the solvent,³⁵ leading to the expulsion of the solvent (water) from the protein matrix. In the framework of Flory-Rehner theory, this can be viewed as a change of the Flory-Huggins interaction parameter χ with temperature. For the muscle-borne protein elastin, the shrinkage behavior with temperature can totally be explained by the variation of χ with temperature.³¹ For elastin, the value of χ doubles approximately, if it is heated from room temperature to 70°C. Above that temperature, χ levels off and stays constant, as protein denaturation has ended. Between room temperature and 70°C, it changes more or less linear.

The muscle protein matrix is a complex of many different proteins, with special proteins crosslinking the myofibers, such as titin and elastin.^{35,36} Hence, during heating of meat also crosslinks can unfold. Unfolding of crosslinks have a twofold effect on swelling behavior: (1) via exposure of hydrophobic parts of the crosslinking proteins the interaction parameter χ changes, and (2) via unfolding the number of crosslinks (ν_c) decreases.³⁷ How the number of crosslinks in muscle meat changes with temperature is not known.

Let us observe the effect of temperature on swelling pressure, assuming a change in the χ parameter only. We take the above-estimated parameter values, but we estimate χ from WHC measurements, as displayed in Figure 2. Below

40°C $\phi \approx 0.2$, and above 80°C $\phi \approx 0.5$. Corresponding with these values $0.56 < \chi < 0.80$. Raw meat has partly denatured via the postmortem process, and hence we can expect χ to be slightly above the value of live muscle tissue $\chi \approx 0.5$. At higher temperature, χ is of comparable order as of elastin ($\chi \approx 1.1$).

In Figure 1, we have plotted the swelling pressure (the difference of osmotic and elastic pressure) as function of the polymer density for different values of χ . The intersection of the curves with $\pi_{sw} = 0$ at $\phi = \phi_e$ indicates equilibrium between osmotic and network pressure. Using different values for M_c does not change much the equilibrium points ϕ_e .

Hence, heating changes the Flory interaction parameter χ , and equilibrium shifts toward higher polymer volume fractions (or lower moisture content). This shift of equilibrium clearly occurs in meat. In meat science, it is said that at certain temperatures, meat can hold only a certain amount of water, which is termed the WHC.³⁶ In Figure 2, WHC of meat is shown, which is expressed in the mass fraction of water.

Near the equilibrium point, we observe that the swelling pressure is linear with the polymer volume fraction, which also follows from a Landau expansion of the free energy functional around the equilibrium point ϕ_e . In our model, we will use this linearization as a constitutive equation for the swelling pressure: $\pi_{sw} \sim (\phi - \phi_e)$.

For meat, it is more natural to speak in terms of moisture content, instead of volume fraction of the protein. The moisture content at equilibrium (when $\pi_{sw} = 0$) is denoted as $n_{eq}(T)$ and will be referred as the WHC in the following. From the linearization around equilibrium thus follows that the swelling pressure is linear with the difference between actual moisture content n (in kg/m³) and WHC:

$$\pi_{sw} = E[n - n_{eq}(T)] \quad (5)$$

Following poroelastic theory, the swelling pressure will be used as the driving potential in Darcy's law.

In earlier studies,^{1,6,39} it is argued that the difference $n - n_{eq}(T)$ is an important quantity in moisture transport of meat and rice. However, Pan and Singh⁶ have used it as a sink term in the mass balance instead of using it as a potential in Darcy's law. Dagerskog¹ has assumed that the moisture content relaxes very fast to the WHC (corresponding with the local temperature). Below we show that this hypothesis is not true.

An objection toward the above model, may be that it is too simplifying, because meat is composed of many different kinds of proteins, which denature at different temperature.³⁵ However, we take the *soft condensed matter* perspective^{13,14} that the swelling behavior of proteins is quite independent of the details of events happening at the microstructural level, as is also hypothesized for muscle fibers by Gosline.³¹ The effects of different denaturing behavior of different proteins are all absorbed in the WHC, which can easily be determined via experiments.

Other studies on swelling of foods^{40,41} have also taken the swelling pressure as the driving potential in a generalized Darcy's law. However, their mathematics is very much involved, and thus difficult to apply to engineering applications such as meat cooking. Furthermore, in their models, no constitutive equation for the swelling pressure is given.

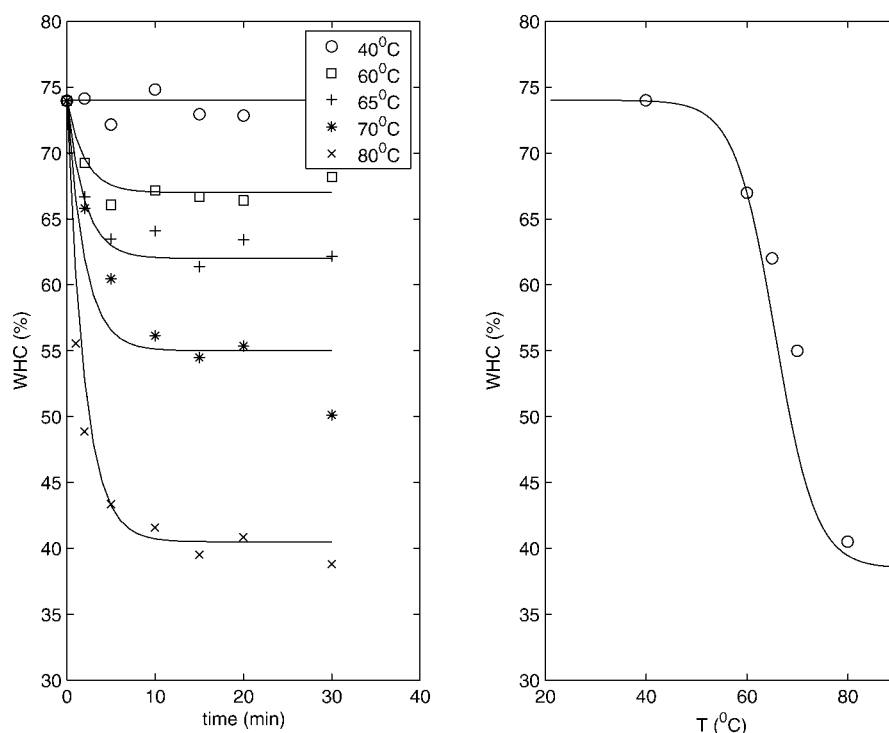


Figure 2. Water holding capacity of beef, expressed as mass fraction of water, as a function of temperature and time.

Experimental data (symbols) are obtained from Bengtson.³⁸ Solid lines are drawn to guide the eye. At the right the final WHC as function of temperature is given, with the fitted sigmoid function.

We gather that the soft matter perspective can be taken further to cooking of other foods. Watanabe and coworkers³⁹ have studied the cooking of rice and used the “water demand” $n - n_{eq}(T)$ as a potential in Ficks law describing moisture migration in the cooking rice. During boiling, the rice temperature stays constant, and in the isothermal case, their model is equivalent with our model, though they have not made a link to the Flory-Rehner theory. The molecular process responsible for change in $n_{eq}(T)$ in cooking rice is starch gelatinization, which is definitely different from protein denaturation—again showing that the details of molecular processes can be absorbed in the WHC.

Jarvis and coworkers⁴² argue that Flory-Rehner theory applies to cooking potatoes, in which starch granules gelatinize inside the potato cells. Here, the cell walls (rich in pectin and cellulose) provide the network pressure restraining the increased osmotic pressure due to gelatinization. They have reported swelling pressures of order 0.1 MPa, which is of comparable order as the swelling pressures in cooking meat.

By reflecting that many foods resemble gels, Mizrahi and coworkers^{24,25} have posed that the sorption in foods at high water activities can be explained by Flory-Rehner theory. They have also stated that Flory-Rehner theory might explain the changes in WHC of foods. The presence of low molecular weight solutes in the food makes the treatment more complex. The direct effect is that the solutes contribute to the osmotic pressure, but they also have indirect effects such as salting-in/salting-out effects, and they can act as cosolutes,

and their interaction with polymers gives extra contributions in the osmotic pressure.⁴³

Model description

To test our hypothesis for liquid moisture transport in cooking meat, we have build a numerical model, describing all relevant heat and moisture flows during cooking of meat at temperatures below boiling point. Above boiling point, internal evaporation occurs, which leads to the formation of a crispy crust. Internal evaporation due to intensive heating like microwave heating leads also to pressure-driven flows,^{8,15,44} but this is due to the nucleation and growing gas or vapor bubbles—whose physics is quite different than the pressure-driven flow due to the protein denaturation. Taking this process into account will increase the complexity of the problem, making it more difficult to validate our hypothesis. This has made us to restrict ourselves to the regime wherein the product temperatures stays below or at wetbulb temperature (which is at maximum at the boiling point of water)—where evaporation only occurs at the surface.

Above all, in fresh meat, the volume fraction of air is very low (about 1%),^{45,46} and hence at temperatures below boiling point the volume increase of the gas phase due to thermal expansion cannot explain the huge expulsion of liquid during cooking of the meat.⁴⁴ Furthermore, as we assume that the gas phase is absent, the model does not contain liquid moisture transport due to capillary pressure gradients.⁴⁴

Next to the above points, we have taken a few further simplifying assumptions:

- Shrinkage of the meat has a negligible effect on heat and moisture flow;
- Meat is assumed not to deform;
- Evaporation occurs only at the surface of the meat;
- Liquid moisture (meat juice) consists of pure water;
- Permeability of the meat is constant, but is anisotropic; and
- Parameter E is independent of temperature.

All assumptions are taken to reduce the complexity of the problem and may not be valid in reality. During cooking, mechanical deformation of the meat can be substantial, and the underlying physics are not that simple, as meat contracts in direction of the fibers, but expands in one of the directions perpendicular to the meat fibers.

In raw meat juice, soluble myoglobin proteins are present and modify the viscosity of the meat juice. At temperatures 40–60°C, they denature and aggregate.³⁵ The amount of myoglobin proteins removed from the meat via the expelled moisture we assume negligible, as they aggregate at temperatures lower than the denaturation temperatures of myofibrillar proteins, which induce the moisture transport. The aggregates we view as part of the biopolymer matrix.

Permeability of the extracellular pore space changes in time due to denaturation of soluble proteins, and collagen of the connective tissues. This is hard to quantify and differentiate from temperature dependency of other model parameters like E . From the above discussion of the Flory-Rehner theory and its linearization around the equilibrium point, it is apparent that E is moderately temperature dependent. This we have found via a very recent review of relatively old literature on the Flory-Rehner theory applied to muscles.^{30,31} Consequently, in the earlier developed numerical model, it is assumed E to be a constant.

Given the above considerations, our model takes into account the following phenomena:

- Moisture transport due to gradients in swelling pressure;
- Evaporation of liquid moisture;
- Heat conduction inside the meat;
- Convective heat transport by the liquid moisture flow;
- Dripping of liquid moisture from the surface; and
- Heat transfer between meat and air flow.

The model can be described in terms of balance equations for energy, momentum, and mass (i.e., moisture). The momentum balance equation reduces to Darcy's law because of the porous medium assumption:

$$\rho_w u = -\frac{\kappa}{\nu} \nabla \pi_{sw} \quad (6)$$

where ρ_w is the bulk density of water, u is the flow velocity, κ is the permeability tensor, and ν is the kinematic viscosity of the fluid. The mass balance equation for the liquid moisture is the continuity equation:

$$\partial_t n + \nabla \rho_w u = 0 \quad (7)$$

and the energy balance equation is

$$\rho_p c_{p,m} \partial_t T + c_{p,w} \nabla \rho_w u T = \lambda_p \nabla^2 T \quad (8)$$

where ρ_p is the mass density of meat, $c_{p,m}$ the specific heat of meat, ρ_w is the mass density of water, $c_{p,w}$ specific heat of

water, T temperature, and λ_m the thermal conductivity of meat. Note that the convective energy flux is transported by the expelled plasma, which is assumed to be pure water.

The model is completed with the boundary conditions. For the energy balance equation, it reads

$$-\lambda_m \partial_n T = h(T - T_0) + r j_{\text{evap}} \quad (9)$$

where h , the mass transfer coefficient and r the latent heat of evaporation, and j_{evap} the mass flux due to evaporation. The evaporative flux is given by

$$j_{\text{evap}} = k(a_w c_{\text{sat}}(T) - c_0) \quad (10)$$

with k , the mass transfer coefficient (linked to the heat transfer coefficient via the Lewis relation). c_0 is the water vapor concentration in the boundary layer above the product, which is in thermal equilibrium with the surface of the meat having temperature T and water activity a_w . k is the mass transfer coefficient, linked to the heat transfer coefficient via the Lewis relation:

$$k = Le^{2/3} h / \rho_a c_{p,a} \quad (11)$$

where ρ_a the density of air, and $c_{p,a}$ the specific heat of air. The Lewis number is defined as $Le = D_a / a_a$, with D_a the diffusion coefficient of water vapor in air, and $a_a = \lambda_a / \rho_a c_{p,a}$ the thermal diffusivity of air.

c_{sat} is the saturated water vapor density, related to the saturation water vapor pressure p_{sat} via the ideal gas law:

$$c_{\text{sat}} = \frac{p_{\text{sat}} M_w}{RT} \quad (12)$$

where M_w is the molar weight of water and R is the gas constant. The saturation water vapor pressure p_{sat} is calculated with the empirical Tetens formula:

$$p_{\text{sat}}(T) = p_{\text{sat},0} \exp\left(17.27 \frac{T - T_0}{T - 35.86}\right) \quad (13)$$

where $p_{\text{sat},0} = 597$ Pa is the vapor pressure at the reference temperature $T_0 = 273.15$ K.

The water activity a_w is dependent on the moisture content n of the surface of the meat. We assume that its behavior is like that of the beef meat.⁴⁷ We have fitted the experimental data of the sorption isotherm with the following approximation of the GAB-isotherm:

$$a_w(1 - X_m/X) \quad (14)$$

where X is the moisture content on dry weight basis, and X_m is the moisture content of the first monolayer of absorbed water. From the experimental study,⁴⁷ it follows that there is little temperature dependency of the water activity for temperatures above 20°C.

The boundary condition for the momentum balance equation (Darcy's law) is that the swelling pressure is zero ($\pi_{sw} = 0$).

For the mass balance equation, the boundary condition is that the mass flux is equal to the sum of flux of the expelled

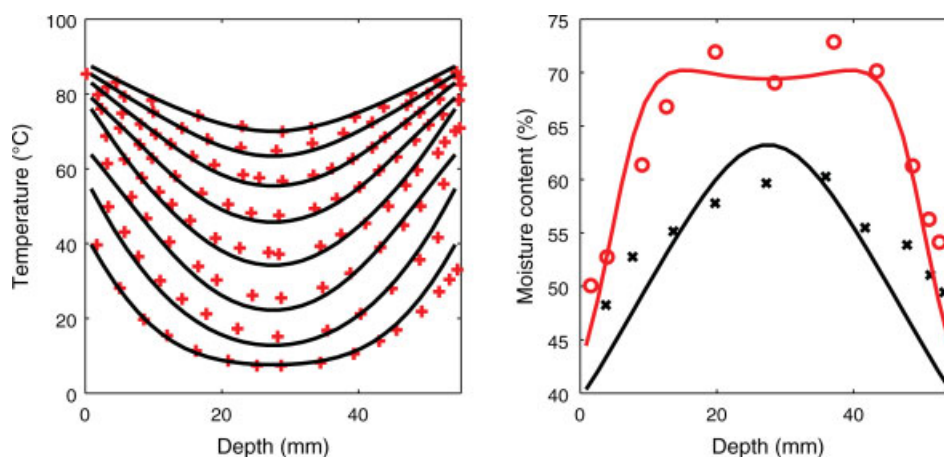


Figure 3. Temperature and moisture profiles during cooking of beef, according to experiment with oven temperature $T_0 = 175^\circ\text{C}$ (symbols) and model (lines).

Temperature profiles are given at a 10-min interval (starting at low temperature), while the moisture profiles are given for cooking times of 40 and 80 min (starting at high moisture content). [Color figure can be viewed in the online issue, which is available at www.interscience.wiley.com.]

liquid moisture and mass flux due to evaporation:

$$\rho_w u = -\frac{\kappa}{v} \partial_n \pi_{sw} + j_{\text{evap}} \quad (15)$$

With the normal derivative of the swelling pressure $\partial_n \pi_{sw}$ computed using the above boundary condition that $\pi_{sw} = 0$ at the surface of the meat. However, via evaporation the swelling pressure can become negative, and in this case we apply a no flux boundary condition for the liquid moisture.

Results and Discussion

Model validation

Using the above model, we analyze the experimental data on roasting a rectangular piece of beef obtained by Bengtson

et al.³⁸ Below, we report on their experimental setup, and the assumptions we have made ourselves.

In the experiment, temperature and moisture profiles are obtained at several times during the cooking process and thus provide a good test for our model. The meat is cooked (roasted) in an oven at air temperatures 175 and 225°C . The duration of the experiment has been 80 and 60 min, respectively. The beef is from the semimembranosus muscle, with a mass of 705 g, and dimensions of $15\text{ cm} \times 8\text{ cm} \times 5.5\text{ cm}$ (length \times width \times height). The meat fibers are parallel to the meat surface, along the length axis of the meat. Initial temperature is 7°C . In the experiment, temperature profiles along the vertical center line, and average moisture content profiles in vertical direction are determined at various times (see Figures 3 and 4). The average moisture profiles are obtained by freezing the cooked meat, and slicing the frozen

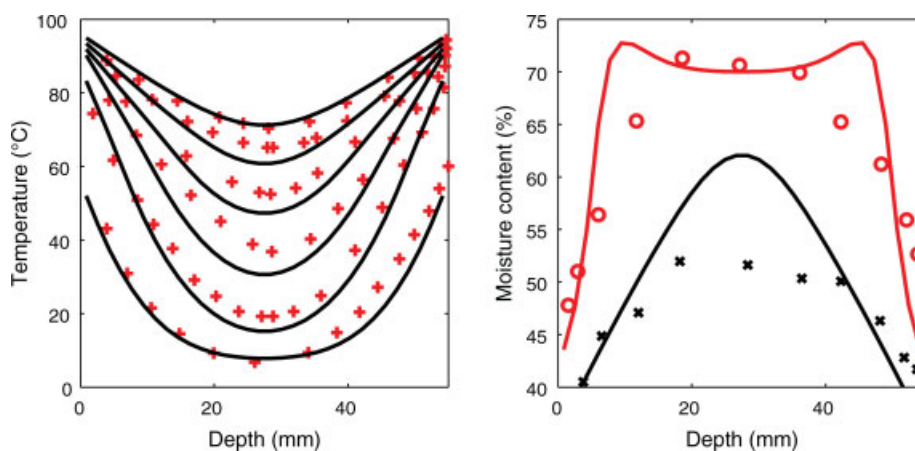


Figure 4. Temperature and moisture profiles during cooking of beef, according to experiment with oven temperature $T_0 = 225^\circ\text{C}$ (symbols) and model (lines).

Temperature profiles are given at a 10-min interval (starting at low temperature), while the moisture profiles are given for cooking times of 30 and 60 min (starting at high moisture content). [Color figure can be viewed in the online issue, which is available at www.interscience.wiley.com.]

meat horizontally, of which the moisture content is determined.

These datasets will be used for our model analysis. During the experiment, the wetbulb temperature of the air changed due to the accumulation of water vapor in the cooking oven. From recordings, it follows that the wetbulb temperature starts at 50°C and increases exponentially in time to about 90°C. Of the actual experiments used for analysis of our model, the wetbulb temperature is not recorded. Hence, we have matched the wetbulb temperature to the recorded surface temperature, as one might assume that the meat surface more or less follows the wetbulb temperature. Consequently, we do not need a high accurate value of the heat transfer coefficient. We take the estimated value of Bengtson et al.,³⁸ namely $h \approx 15 \text{ W/m}^2 \text{ K}$

Also, the water content of thin slices (2 mm) of the beef put in constant temperature water baths has been measured as a function of time and temperature by Bengtson et al.³⁸ It is found that after 10 min more or less stable values of the water content have been obtained, which can be viewed as the WHC. We have repeated the experimental data in Figure 2. We view that the dynamics in water content are *not* due to slow kinetics of protein denaturation, but due to slow relaxation of the protein matrix (because the moisture has to be expelled), and thus are already captured by our model. The time scale of denaturation for isolated proteins is in the order of several seconds, as is found for myosin in hake.⁴⁸ The (averaged) experimental values for times larger than 30 min we take as the equilibrium values of the WHC $n_{\text{eq}}(T)$.

The experimental data of n_{eq} we have fitted to a sigmoid function:

$$n_{\text{eq}}(T) = 0.74 - \frac{0.345}{1 + 30 \exp[-0.25(T - T_\sigma)]} \quad (16)$$

with $T_\sigma = 325 \text{ K} = 52^\circ\text{C}$ the center of the sigmoid curve. The fitted curve is shown in Figure 2.

From the sorption data of Delgado, we have estimated X_m , the monolayer moisture content. Using nonlinear regression, we have found that $X_m = 0.08$, which is in agreement with the value of $X_m = 0.085$ obtained by fitting the full GAB-equation to the data.³⁸

The thermophysical properties of the meat are computed from its composition, as expressed in mass fractions of water $y_w = 0.74$ and of proteins $y_p = 0.26$.^{49,50} The specific heat of the beef is

$$c_{p,m} = y_w c_{p,w}(T) + y_p c_{p,p}(T) \quad (17)$$

where $c_{p,w}$ the specific heat of water and $c_{p,p}$ the specific heat of proteins.

For the thermal conductivity of the beef, we take into account the anisotropy due to the parallel orientation of the meat fibers.⁵¹ Thermal conductivity parallel to the fibers is computed using the parallel model:

$$\lambda_{m,\parallel} = \phi_w \lambda_w + \phi_p \lambda_p \quad (18)$$

and the thermal conductivity perpendicular to the fibers is computed using the series model:

$$\frac{1}{\lambda_{m,\perp}} = \frac{\phi_w}{\lambda_w} + \frac{\phi_p}{\lambda_p} \quad (19)$$

where $\phi_w = y_w \rho_m / \rho_w$ and $\phi_p = y_p \rho_m / \rho_p$ are the volume fractions of water and proteins, respectively, with ρ_w and ρ_p the bulk densities of water and proteins and $1/\rho_m = y_w/\rho_w + y_p/\rho_p$.

At initial temperature, we find $\lambda_{m,\parallel} = 0.500 \text{ W/m}^2 \text{ K}$ and $\lambda_{m,\perp} = 0.404 \text{ W/m}^2 \text{ K}$. Because moisture transports the mass fractions, y_w and y_p will change, and hence we have to relate the moisture density n to the mass fraction: $n = y_w \rho_m$. The parallel orientation of the meat fibers also gives anisotropy in permeability κ . It is stated that the resistance to moisture transport perpendicular to the fibers is 1.2 times higher than the resistance to moisture transport parallel to the fibers,⁵¹ hence $\kappa_{\parallel} = 1.2 \kappa_{\perp}$.

From the analysis, follows that there is one single unknown parameter, namely the product $\gamma = \kappa_{\parallel} E / v$, which has the units of a diffusion coefficient. From the Landau expansion of the Flory-Rehner expression for the swelling pressure, follows that at $T = 70^\circ\text{C}$, $E \approx 10^4 \text{ (Pa m}^3/\text{kg)}$. In the meat juice, some soluble proteins can be present, lowering the viscosity. The lower limit for the viscosity is that of water $\nu \approx 10^{-6} \text{ m}^2/\text{s}$. Datta⁵² has performed experimental determination of the permeability of raw beef, obtaining $\kappa_{\parallel} \approx 10^{-17} \dots 10^{-19} \text{ m}^2$. Hence, we expect that $\gamma \approx 10^{-9} \dots 10^{-6} \text{ m}^2/\text{s}$.

Scale analysis

We perform scale analysis to investigate whether the complexity of the model can be further reduced for the problem of the roasted beef. As scales we will use the thickness of the piece of beef L_z , the cooking time t_e , the pressure scale $P_{\text{max}} = E(n_w(t=0) - n^{\text{eq}}(T = 70^\circ\text{C}))$, the velocity scale $U = P_{\text{max}}/(\rho_w L_z)$. The temperature scales between $10^\circ\text{C} < T < 90^\circ\text{C}$, and the water density scales between $n_{\text{eq}}(T = 90^\circ\text{C}) < n < n(t=0)$. The rescaled variables are

$$\hat{x}_z = x_z / L_z ; \hat{t} = t / \tau_D ; \hat{u} = u / U ; \hat{\pi} = \pi_{\text{sw}} / P_{\text{max}} \quad (20)$$

with the diffusive time scale $\tau_D = L_z^2 / \alpha_p$ and the thermal diffusivity $\alpha_p = \lambda_p / \rho_p c_{p,p}$. The reduced temperature and water density are

$$\hat{T} = \frac{T - T_{\text{init}}}{T_{\text{dew}} - T_{\text{init}}} ; \quad \hat{n} = \frac{n - n_{\text{eq,min}}}{n_{\text{init}} - n_{\text{eq,min}}} \quad (21)$$

Before scaling the mass balance, we substitute Darcy's law Eq. 6 into the continuity Eq. 7. Furthermore, we apply the product rule to $\nabla(n - n_{\text{eq}})$, as the WHC is temperature dependent. The resulting equation is mathematically similar to the Luikov model¹⁹:

$$\partial_t n = -\gamma \nabla^2 n - \gamma \nabla \frac{\partial n_{\text{eq}}(T)}{\partial T} \nabla T \quad (22)$$

with $\gamma = E \kappa / \nu \approx 10^{-7} \text{ m}^2/\text{s}$.

Dropping the hat symbols for all dimensionless variables, we obtain the rescaled energy and mass balance equations:

$$\partial_t T + Pe \nabla u T = \nabla^2 T \quad (23)$$

$$\partial_t n = -De [\nabla^2 n - Xc \nabla \partial_T n_{eq} \nabla T] \quad (24)$$

Hence, there are three governing dimensionless numbers, with the Peclet number:

$$Pe = \frac{c_{p,w} \rho_w UL_z}{\lambda_p} = \frac{UL_z}{\alpha} \quad (25)$$

(with α the thermal diffusivity). The Deborah number is:

$$De = \frac{\tau_D L_z^2}{\gamma} \quad (26)$$

and the coupling constant is:

$$Xc = \frac{n_{init} - n_{eq,min}}{T_{dew} - T_{init}} \quad (27)$$

Using the above-estimated values of the various scales, we have calculated the order of magnitude of the dimensionless numbers. We have obtained $Pe \approx 10^{-1}$, $De \approx 10^0$, $Xc \approx 10^0$. Hence, we expect all terms in the governing equations to be significant. As the time scale of heat conduction and moisture transport are comparable $De \approx 1$, one can *not* make the assumption that $n = n_{eq}(T)$ as proposed by Dagerskog.¹

Numerical analysis

The above model we have discretized following the cell centered Finite Volume method on a rectangular grid, having $8 \times 8 \times 16$ control volumes. As we assume uniform heat transfer coefficient, there is mirror symmetry in x , y , and z planes, and consequently, we have applied symmetry boundary conditions at these midplanes. This renders grid spacings of $\Delta x = 9.4$ mm, $\Delta y = 5.0$ mm, and $\Delta z = 1.7$ mm. For the time discretization, we have applied Euler forward, and for the spatial derivatives central differencing. As the Peclet number $Pe \approx 0.1$, the grid Peclet number $Pe^* = \tau_D U \Delta x \ll 2$, and, consequently, we expect no numerical dispersion problems with central differencing applied to the convection diffusion equation.

Parameter estimation of $\gamma = \kappa_{||} E / v$ is performed via minimization of the L_2 norm between predictions of temperature and moisture profiles. We have found that L_2 norm is minimal for $\gamma = 0.1 \cdot 10^{-6}$ m²/s, which is within the estimated order of magnitude as given earlier.

Predictions using this parameter value are shown in Figures 3 and 4, together with the experimental data for the temperature and moisture profiles. Moisture content is expressed as a mass fraction y_w . The temperature profiles are given at a 10-min time interval. The moisture profile is obtained after 40 and 80 min in case of $T_0 = 175^\circ\text{C}$, and after 20 and 60 min in case of $T_0 = 225^\circ\text{C}$. From the figures, we observe that the model predictions and experimental data compare quite well. On the basis of these results, we assume our model—based on the linearization of Flory-Rehner theory—to be valid.

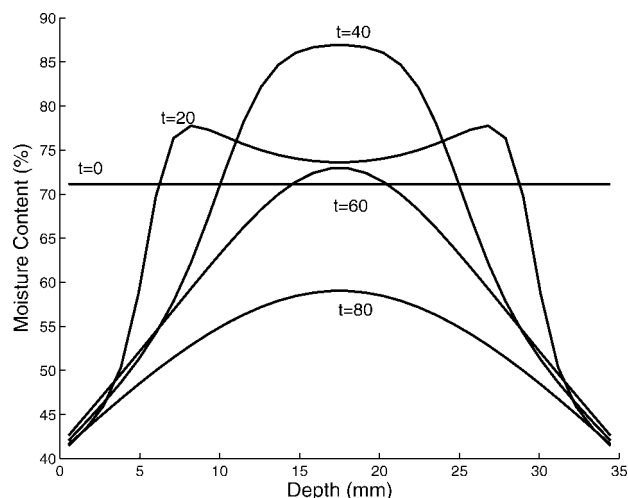


Figure 5. Moisture profile at center line, as function of time and height.

With time t given in minutes.

Detailed physics of moisture migration

After having validated the model against experimental data, we explore the physics occurring during cooking in more detail—and the rise of the moisture content in the center of the meat in particular. We have observed this phenomenon during trial simulations and found that this has been observed experimentally^{10,18}—but has not been explained until very recently in the independent study of Tornberg and coworkers,¹² who give a similar account of the phenomenon as below.

We have simulated the cooking of a rectangular piece of beef with same properties as earlier, but now we have assumed (1) a height of 35 mm, (2) a constant dewpoint temperature of $T_{dew} = 85^\circ\text{C}$, and (3) an oven temperature of $T_0 = 175^\circ\text{C}$. We examine the moisture content profile along the vertical central axis of the beef for the first 80 min of cooking. The profiles at times $t = 0, 20, 40, 60$, and 80 min are shown in Figure 5. We observe that the moisture content is rising in the center of the piece of beef. The time scale and the relative increase of moisture content is quite comparable with NIR observations¹⁸ (on meat pieces of thickness 20 mm but unknown width and length), wherein one has found a rise of moisture content above the initial value for 40 min. The initial moisture content is 65%, and the maximal moisture content is 75% (expressed as mass fractions). Our model predictions are of comparable order.

This rise can be quite well explained by the investigation of the swelling pressure profile, as shown in Figure 6. In the first 20 min of the heating only the subsurface of the meat is above the denaturation temperature (see Figure 7), and hence there is an increase of the swelling pressure, while in the central region the swelling pressure remains about zero. Consequently, next to the pressure gradient between surface and subsurface, there is a pressure gradient between the subsurface and the central region, and as stated by Darcy's law this leads to a moisture flow *towards* the central region. This inward moisture flow increases the moisture content of the central region.

After 20 min also the central region rises above the denaturation temperature, and the swelling pressure increases rapidly (due to temperature increase, the moisture content becomes increasingly larger than the equilibrium value n_{eq}). Shortly after 40 min, the swelling pressure will be maximal in the central region. After that, there will be only outward moisture flow, and the moisture content in the central region will fall.

We note that the existence of a significant swelling pressure (in the order of 0.3 MPa), which is proportional to $n - n_{eq}(T)$, indicates again that actual moisture content is very different from the equilibrium moisture content (WHC).

Model extensions

In many ways, our model presented earlier simplifies part of the physics during meat cooking, though it can predict temperature and moisture transport in the above-mentioned experiment with reasonable accuracy. We imagine that for (1) conditions with lower dewpoint or higher oven temperature, or (2) smaller pieces of meat, we have to alleviate some of these simplifications. Below, we discuss some of these points, which can serve as new directions of future research.

During intensive heating processes such as microwave, frying, and roasting, evaporation occurs not only at the surface. An evaporation front will move into the meat, and moisture transport via the gas phase has to be included. A class of food heating models includes the gas transport, and which can be incorporated straightforward in the above-mentioned model, have been developed by Datta and coworkers.^{15,16}

Another extension of the model is the incorporation of the shrinkage of the meat. The physics of this process is well known, and is found in the literature of poroelastic theory.^{23,26} Numerical implementation can be a hurdle, as most of the models describing mechanical deformation of

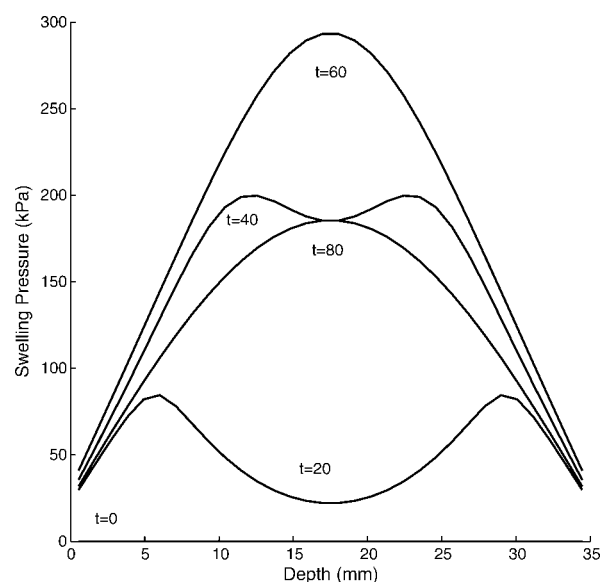


Figure 6. Swelling pressure profile at center line, as function of time and height.

Time t is given in minutes.

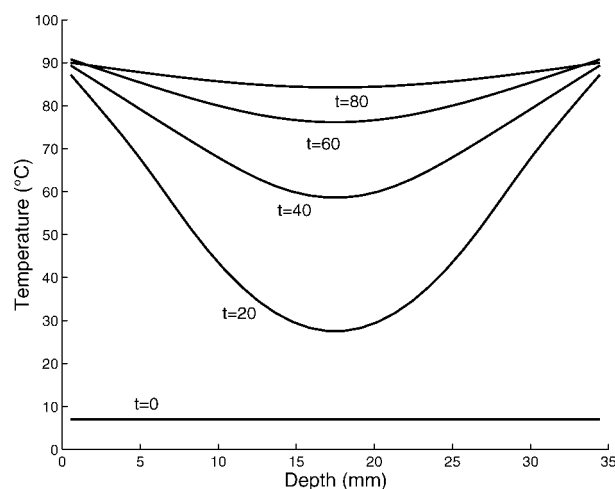


Figure 7. Temperature profile at center line, as function of time and height.

Time t is given in minutes.

poroelastic media are formulated in the framework of Finite Elements, while mass, momentum, and energy transport are more naturally formulated in the framework of Finite Volume Method, as applied in the above-mentioned numerical model.

During heating of smaller pieces of meat, dynamics in the permeability might become important to consider. In the review of Tornberg,³⁵ it is stated that the extracellular channels undergo significant changes in width during cooking, as reported in more detail in the introduction and also by Palka.^{53,54} They have reported granulation and subsequent gelatinization of denaturated collagen in the extracellular channels, which is also found during heating of fish.⁴⁸ As moisture transport is mainly through the extracellular channels, the above-mentioned dynamics will effect the permeability of the protein matrix.

Conclusions

As one can observe from our results, the numerical predictions and experimental data³⁸ compare quite well, for both analyzed heating experiments. Hence, this gives us much confidence that our description of liquid moisture flow based on the linearized Flory-Rehner theory is a valid model for this process and provides the framework for incorporating more physics as moisture transport during brining and curing of meat, in which transport of ions is significant.

Despite its simplifications, our model definitely shows the potential of the *soft condensed matter* perspective on meat cooking. The *soft condensed matter* perspective on moisture transport during cooking seems to hold for many types of gel-like foods such as rice and potatoes. In essence, the *soft matter perspective* comprises (1) the driving potential (swelling pressure) for moisture transport is derived from a free energy functional, like the Flory-Rehner functional, and (2) the free energy functional is much independent of the molecular details of the biopolymer matrix. The driving potential is to be inserted in transport equations following the porous media approach.^{8,40,41}

Literature Cited

- Dagerskog M. Pan frying of meat patties. I. A study of heat and mass transfer. *Lebensm.-Wiss. u. Technol.* 1979;12:217–224.
- Fowler AJ, Bejan A. The effect of shrinkage on the cooking of meat. *Int. J. Heat Fluid Flow.* 1991;12: 375–382.
- Huang E, Mittal GS. Meatball cooking—modeling and simulation. *J. Food Eng.* 1995;24:87–100.
- Ngadi MO, Watts KC, Correia LR. Finite element method modelling of moisture transfer in chicken drum during deep-fat frying. *J. Food Eng.* 1997;32:11–20.
- Chen H, Marks BP, Murphy RY. Modeling coupled heat and mass transfer for convection cooking of chicken patties. *J. Food Eng.* 1999; 42:139–146.
- Pan Z, Singh RP, Rumsey TR. Predictive modelling of contact-heating process for cooking a hamburger patty. *J. Food Eng.* 2000;46: 9–19.
- Shilton N, Mallikarajan P, Sheridan P. Modelling of heat transfer and evaporative mass losses during the cooking of beef patties using far-infrared radiation. *J. Food Eng.* 2002;55:217–222.
- Datta AK. Porous media approaches to studying simultaneous heat and mass transfer in food processes. I. Problem formulations. *J. Food Eng.* 2007;80:80–95.
- Gekas V. Mass transfer modeling. *J. Food Eng.* 2001;49:97–102.
- Wahlby U, Skjoldstrand C. NIR-measurements of moisture changes in foods. *J. Food Eng.* 2001;47:303–312.
- Godsalve EW, Davis EA, Gordon J. Water loss rates and temperature profiles of dry cooked bovine muscle. *J. Food Sci.* 1977;42:1038–1045.
- Oroszvari BK, Bayod E, Sjöholm I, Tornberg E. The mechanisms controlling heat and mass transfer on frying of beefburgers. III. Mass transfer evolution during frying. *J. Food Eng.* 2006;76:169–178.
- Donald AM. Physics of foodstuffs. *Rep. Prog. Phys.* 1994;57:1081–1135.
- Mezzenga R, Schurtenberger P, Burbidge A, Miche M. Understanding foods as soft materials. *Nat. Mater.* 2005;4:729–740.
- Ni H, Datta AK, Torrance KE. Moisture transport in intensive microwave heating of biomaterials: a multiphase porous media model. *Int. J. Heat Mass Transf.* 1999;42:1501–1512.
- Zhang J, Datta AK, Mukherjee S. Transport processes and large deformation during baking of bread. *AIChE J.* 2005;51:2569–2580.
- Bell JW, Farkas BE, Hal SA, Lanier TC. Effect of thermal treatment on moisture transport during steam cooking of skipjack tuna (*Katsuwonus pelamis*). *J. Food Sci.* 2001;66:307–313.
- Thorvaldsson K, Skjoldstrand C. Water transport in meat during reheating. *J. Food Eng.* 1996;29:13–21.
- Irudayaraj J, Wu Y. Numerical modeling of heat and mass transfer in starch systems. *Trans. ASAE.* 1999;42:449–455.
- van Dijk HJM, Walstra P. Syneresis of curd I. General considerations and literature review. *Neth. Dairy J.* 1985;39:209–246.
- van Dijk HJM, Walstra P. Syneresis of curd. II. One dimensional syneresis of rennet curd in constant conditions. *Neth. Dairy J.* 1986;40:3–30.
- Tijssens E, de Baerdemaeker J. Mathematical modelling of syneresis of cheese curd. *Math. Comput. Simulat.* 2004;65:165–175.
- Wu S, Li H, Chen JP, Lam KY. Modeling investigation of hydrogel volume transition. *Macromol. Theory Simulat.* 2004;13:13–29.
- Mizrahi S, Eichler S, Ramon O. Osmotic dehydration phenomena in gel systems. *J. Food Eng.* 2001;49:87–96.
- Eichler S, Ramon O, Cohen Y, Mizrahi S. Swelling and contraction driven mass transfer processes during osmotic dehydration of uncharged hydrogels. *Int. J. Food Sci. Technol.* 2002;37:245–253.
- Barriere B, Leibler L. Kinetics of solvent absorption and permeation through a highly swellable Elastomeric network. *J. Polym. Sci. B* 2003;41:166–182.
- van der Graaf S, Nisisako T, Schroen CGPH, van der Sman RGM, Boom RM. Lattice Boltzmann simulations of droplet formation in a T-shaped microchannel. *Langmuir* 2006;22:4144–4152.
- van der Sman RGM, van der Graaf S. Diffuse interface model of surfactant adsorption onto flat and droplet interfaces. *Rheol. Acta.* 2006;46:3–11.
- Hill TL. Some statistical mechanical models of elastic polyelectrolytes and proteins. *J. Chem. Phys.* 1952;20:1259–1273.
- van Kleef FSM, Boskamp JV, van den Tempel M. Determination of the number of cross-links in a protein gel from its mechanical and swelling properties. *Biopolymers* 1978;17:223–235.
- Gosline JM. The temperature-dependent swelling of elastin. *Biopolymers* 1978;17:697–707.
- Maughan DW, Godt RE. A quantitative analysis of elastic, entropic, electrostatic, and osmotic forces within relaxed skinned muscle fibres. *Biophys. Struct. Mech.* 1980;7:17–40.
- Regini JW, Elliott GF. The effect of temperature on the donnan potentials in biological polyelectrolyte gels: cornea and striated muscle. *Int. J. Biol. Macromol.* 2001;28:245–254.
- Farhat IA, Blanshard JMV. On the extrapolation of the melting temperature of dry starch from starch-water data using the Flory-Huggins equation. *Carbohydr. Polym.* 1997;34:263–265.
- Tornberg E. Effect of heat on meat proteins—implications on structure and quality of meat products. *Meat Sci.* 2005;70:493–508.
- Offer G, Knight P, Jeacocke R, Almond R, Cousins T, Elsey J, Parsons N, Sharp A, Starr R, Purslow P. The structural basis of the water-holding, appearance and toughness of meat and meat products. *Food Microstr.* 1989;8:151–170.
- Dušek K, Dušková-Smrčková M, Ilavský M, Stewart R, Kopeček J. Swelling pressure induced phase-volume transition in hybrid biopolymer gels caused by unfolding of folded crosslinks: a model. *Biomacromolecules* 2003;4:1818–1826.
- Bengtson NE, Jakobsson B, Dagerskog M. Cooking of beef by oven roasting: a study of heat and mass transfer. *J. Food Sci.* 1976;41:1047–1053.
- Watanabe H, Fukuoka M, Tomiya A, Mihori T. A new non-Fickian diffusion model for water migration in starchy food during cooking. *J. Food Eng.* 2001;49:1–6.
- Achanta S, Okos MR, Cushman JH, Kessler DP. Moisture transport in shrinking gels during saturated drying. *AIChE J.* 1997;43:2112–2122.
- Singh PP, Cushman JH, Maier DE. Multiscale fluid transport theory for swelling biopolymers. *Chem. Eng. Sci.* 2003;58:2409–2419.
- Jarvis MC, MacKenzie E, Duncan HJ. The textural analysis of cooked potato. II. Swelling pressure of starch during gelatinization. *Potato Res.* 1992;35:93–102.
- Livney YD, Portmays I, Faupin B, Fahoum L, Ramon O, Cohen Y, Mizrahi S, Cogan U. Interactions of glucose and polyacrylamide in solutions and gels. *J. Polym. Sci. B* 2003;41:3053–3063.
- Constant T, Moyne C, Perre P. Drying with internal heat generation: theoretical aspects and application to microwave heating. *AIChE J.* 1996;42:359–368.
- MacDonald K, Sun DW. The formation of pores and their effect in a cooked beef product on the efficiency of vacuum cooling. *J. Food Eng.* 2001;47:175–183.
- Deumier F, Trystram G, Collignan A, Guedider L, Bohuon P. Pulsed vacuum brining of poultry meat: interpretation of mass transfer mechanisms. *J. Food Eng.* 2003;58:85–93.
- Delgado AE, Sun DW. Desorption isotherms for cooked and cured beef and pork. *J. Food Eng.* 2002;51:163–170.
- Beas VE, Wagner JR, Anon MC, Crupkin M. Thermal denaturation in fish muscle proteins during gelling: effect of spawning condition. *J. Food Sci.* 1991;56:281–284.
- Singh RP, Heldman DR. *Introduction to Food Engineering*, 2nd ed. San Diego: Academic Press, 1993.
- Choi Y, Okos MR. Effect of temperature and composition on the thermal properties of foods. In: Weisser H, Le Maguer M, Jelen P, editors. *Food Engineering and Process Applications*. Elsevier: New York, 1996:93–98.
- Sun DW, Hu Z. CFD predicting the effects of various parameters on core temperature and weight loss profiles of cooked meat during vacuum cooling. *Comput. Elec. Agric.* 2002;34:111–127.
- Datta AK. Hydraulic permeability of food tissues. *Int. J. Food Prop.* 2006;9:767–780.
- Palka K. Changes in intramuscular connective tissue and collagen solubility of bovine *m. semitendinosus* during retorting. *Meat Sci.* 1999;53: 189–194.
- Palka K, Daun H. Changes in texture, cooking loss, and myofibrillar structure of bovine *m. semitendinosus* during retorting. *Meat Sci.* 1999;51:237–243.

Manuscript received Aug. 14, 2006, and revision received Aug. 22, 2007.